Fully Printed Sensors for In Situ Temperature, Heat Flow, and Thermal Conductivity Measurements in Flexible Devices

Florian Le Goupil, Guillaume Payrot, Sokha Khiev, Wiljan Smaal, Georges Hadziioannou

Fully printed sensors for in-situ temperature, heat flow and thermal conductivity measurements in flexible devices.

Florian Le Goupil[1,], Guillaume Payrot[2], Sokha Khiev[2], Wiljan Smaal[2], and Georges Hadziioannou[1,2,*]*

[1] Laboratoire de Chimie des Polymères Organiques (LCPO UMR 5629), Université de Bordeaux, CNRS, Bordeaux INP, 16 Avenue Pey-Berland, 33607 Pessac Cedex, France

[2] ELORPrintTec, Allée Geoffroy Saint-Hilaire, F-33600, Pessac, France

Email: florian.le-goupil@u-bordeaux.fr, georges.hadziioannou@u-bordeaux.fr

KEYWORDS: temperature sensor, printed electronics, flexible substrate, screen printing, thermal conductivity

ABSTRACT**: Flexible temperature sensors allow temperature monitoring in wearable healthcare devices. A temperature sensor, which can be printed on flexible substrates, is designed and fabricated using a low-cost silver particle ink and a fast and scalable screen-printing process. A high temperature resolution of 10 m°C is reached. The versatility of this temperature sensor design is demonstrated for various applications, including in-situ heat flux measurements, where a 2 mW cm^{-2} resolution is reached, and thermal conductivity measurements on polymer films as thin as 25 µm, with a wide range of accessible values from ~ 0.1 to 0.8 W K^{-1} m^{-1}.**

INTRODUCTION

Printed electronics is widely regarded as the route toward cheap, large-area, flexible and easily scalable electronics.[1] Carbon-based circuit boards including transistors, capacitors and resistors can now be printed with competitive performance. However, the extra temperature sensitivity resulting from their organic nature has made thermal management in these components all the more critical. Temperature sensors, which are printable on flexible substrates, can help monitor the temperature and heat flux inside organic circuit-boards and identify the potentially over-heating areas. In addition to thermal management, these printable sensors can be used in wearable electronics for healthcare, where the monitoring of human body temperature is especially important as minimal changes lead to drastic effects on the metabolism.[2] Printed temperature sensors can even be used to quantify the performance of newly developed cooling devices such as thermo-electric or electrocaloric coolers[3], where direct in-situ measurements of heat flux are needed. Due to these growing interest, the number of publications on flexible sensors has increased three-fold over the last ten years.[2,4–7] These flexible temperature sensors are mostly resistance temperature sensors, which rely on the strong temperature dependence of their electrical resistance. Typical flexible resistance temperature sensors use expensive inorganic metals, such as platinum or gold, either as coating produced by deposition, evaporation or sputtering,[8–10] or through printable inks containing metallic micro- or nano-objects (particles, wires, …).[11,12] Also used are insulating or semi-conducting polymer matrices, such as poly(3,4-ethylene dioxythiophene)-poly(styrene sulfonate), in which thermally conducting loads, such as carbon black or carbon nano-tubes, have been added.[2,13] Printing techniques including screen-printing[14,15] or ink-jet printing[16–18] can then be used to print various materials on flexible substrates.

Here, we report a fully printed resistance temperature sensor using silver particles. Silver inks offer a cheap (< 10 \$ g^{-1}) alternative to expensive commercial platinum sensors and are

compatible with the easily-scalable screen-printing technique. Printed silver-based sensors have been reported to display good performance, with sensitivity values close to that of platinum-based sensors (> 0.2 % °C),[2,8,19] building on the sensitivity of bulk silver (0.38 % °C).[7] However, they are still unable to reach the state-of-the-art temperature resolutions (< 0.1°C) recently reported in sensors with more complex architectures, such as designs using reduced graphene oxide.[20,21] By combining a highly-sensitive micro-pattern obtained using scalable screen-printing with an advanced signal treatment, we reach a 10 m°C thermal resolution. As a result, the temperature sensors can be used for in-situ heat flux measurements, with a 2 mW cm^{-2} resolution, and thermal conductivity measurements on polymer films as thin as 25 µm.

RESULTS AND DISCUSSION

The temperature sensors consist of a conductive line of silver particles arranged to maximize the length of the line, and thus the resistance, in the sensing area by using a meandering pattern, as shown in Fig. 1a. The temperature sensing mechanisms of the sensor relies on the increase of the electronic resistivity of a metallic conductor (silver here), with increasing temperature. This results from the increase of molecular vibrations, which hinder the movement of free electrons. The silver line width was set to 300 µm, while the overall sensing area was 2.3 cm^{-2}. Wider silver pads were printed outside the sensing area for the electrical connection to the data acquisition system. A low-cost commercial silver ink was screen-printed in the desired pattern (printing protocol in Supporting Information). This design of temperature sensor was printed successfully on various flexible substrates, including poly(ethylene terephthalate) (PET) as shown in Fig. 1b, as well as poly(ethylene naphthalate) (PEN) and polyimide (PI). A homogeneous silver particle conductive line with a width of 300 µm was obtained after only one run of screen-printing, as confirmed by the scanning electron microscope macrograph displayed in Fig. 1c. In addition to its compatibility with roll-to-roll processes, and thus its

scalability, screen-printing is a fast process, which allows the printing of the pattern in ~ 1 min in a sheet-to-sheet process. With a large screen, several devices can be printed simultaneously without increasing the production duration, which is a great advantage compared to other technologies such as ink-jet, which generally have a lower throughput.

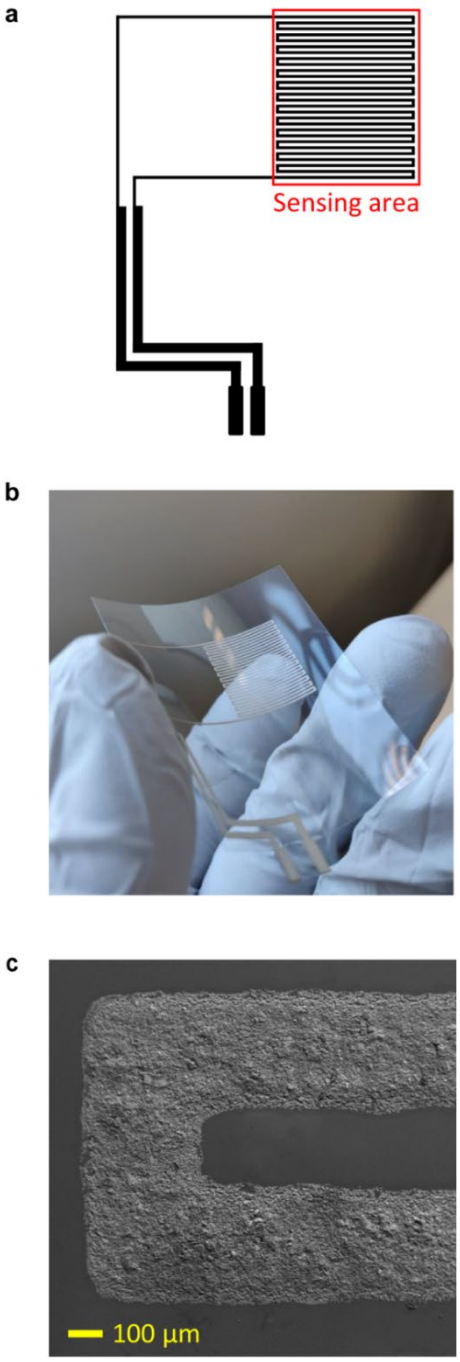

Figure 1. **a)** Schematic representation of the temperature sensor. **b**) Optical image of the temperature sensor screen-printed on a flexible PET substrate. **c)** Scanning electron microscope micrograph of the silver particle conductive line of the printed temperature sensor (magnification x75).

The resistance of the temperature sensors (R_2) was characterised using a voltage divider represented schematically in the insert of Fig. 2a. The temperature sensor is placed in series with a resistor of known resistance (R_1) and the output Voltage U_2 is measured for a given input Voltage U so that

$$R_2 = \frac{U_2\, R_1}{U - U_2}$$

U_2 was recorded with a 16-bit analog-to-numeric converter. The evolution with temperature of the resistance of the temperature sensor is displayed in Fig. 2a. from 22 °C to 40 °C, which includes the temperature range of interest for body temperature monitoring (36 °C to 40 °C).[4] It shows that a 1 °C change of temperature corresponds to a change of 287 mΩ in resistance (dR/dT). This resolution is better than recently reported values for a similar system of dR/dT = 109 mΩ $°C^{-1}$, due to our decreased silver line width of 300 µm, compared to 500 µm used by Liew et al.[18] This resolution could be further enhanced by increasing the overall surface area of the temperature sensors, which would increase the overall length of the silver resistance temperature sensor. However, we decided to use a small surface area (2.3 cm^{-2}) for a wider variety of possible applications. Further improvement could also be obtained with thinner resistance temperature sensors, but decreasing the line width < 300 µm proved detrimental to the quality of the patterns produced by screen-printing. Alternatively, inkjet printing could produce thinner lines and be used to print similar types of silver resistance temperature sensors.[17,22,23] However, screen-printed was favored due to its aforementioned higher fabrication speed and scalability.

The most common tool to quantify the resolution of such sensors is the temperature coefficient of resistance (*TCR*), also sometimes referred to as temperature sensitivity (*S*), defined as:

$$TCR = \frac{1}{R_0}\,\frac{R - R_0}{T - T_0}$$

TCR = 0.25 % $°C^{-1}$ was measured for our printed temperature sensor with reference temperature T_0 = 22 °C. This is comparable to the *TCR* of reference platinum temperature sensors (*TCR* = 0.2 – 0.4 % $°C^{-1}$), while offering a much cheaper alternative.[2,8] While the potential oxidation of silver could eventually result in poor long-term stability of the sensors; their use for in-situ measurements, as proposed here, or healthcare applications, would require them to be buried inside a larger sealed structure or encapsulated, thus preventing their oxidation.

Building on this promising *TCR*, a high thermal resolution of 10 m°C was targeted for this printed temperature sensor. Instead of further increasing the *TCR*, this was achieved by reaching a resistance resolution of 3 mΩ (as dR/dT ~ 0.3 Ω $°C^{-1}$), through the optimization of U and R_1 for the advanced data acquisition of the 16 bit analog-to-numeric converter as well as the use of a moving average signal "treatment".

A small set-up was designed to study the influence of the temperature sensor's resistance resolution on its temperature and heat-flux measurement capabilities. Two temperature sensors were screen-printed on a 75-µm-thick PET substrate, with one on each side and overlapping sensing areas. They were then inserted between a Peltier heater and a thick (6 mm) aluminium heat sink, using 50-µm-thick polyimide tape for electrical insulation between each layer, as shown in Fig. 2b. The whole stack was then thermally insulated using a polylactic acid (PLA) box tailor-made by 3D-printing.

The resistance resolution was first decreased down to 10 mΩ by stabilizing U and optimizing R_1. U was applied using a constant voltage source with a voltage stability down to a few microVolts in order to avoid additional parasitic noise from the voltage source during the resistance data acquisition. The reference resistance R_1 was then set to 1580 Ω in order to keep it high enough for the overall current flowing through the circuit to remain below 10 mA (highest current supported by the constant voltage source), but also as low as possible to reach the highest resolution available with our choice of analog-to-digital converter (see supporting information for more details, Fig. S1).

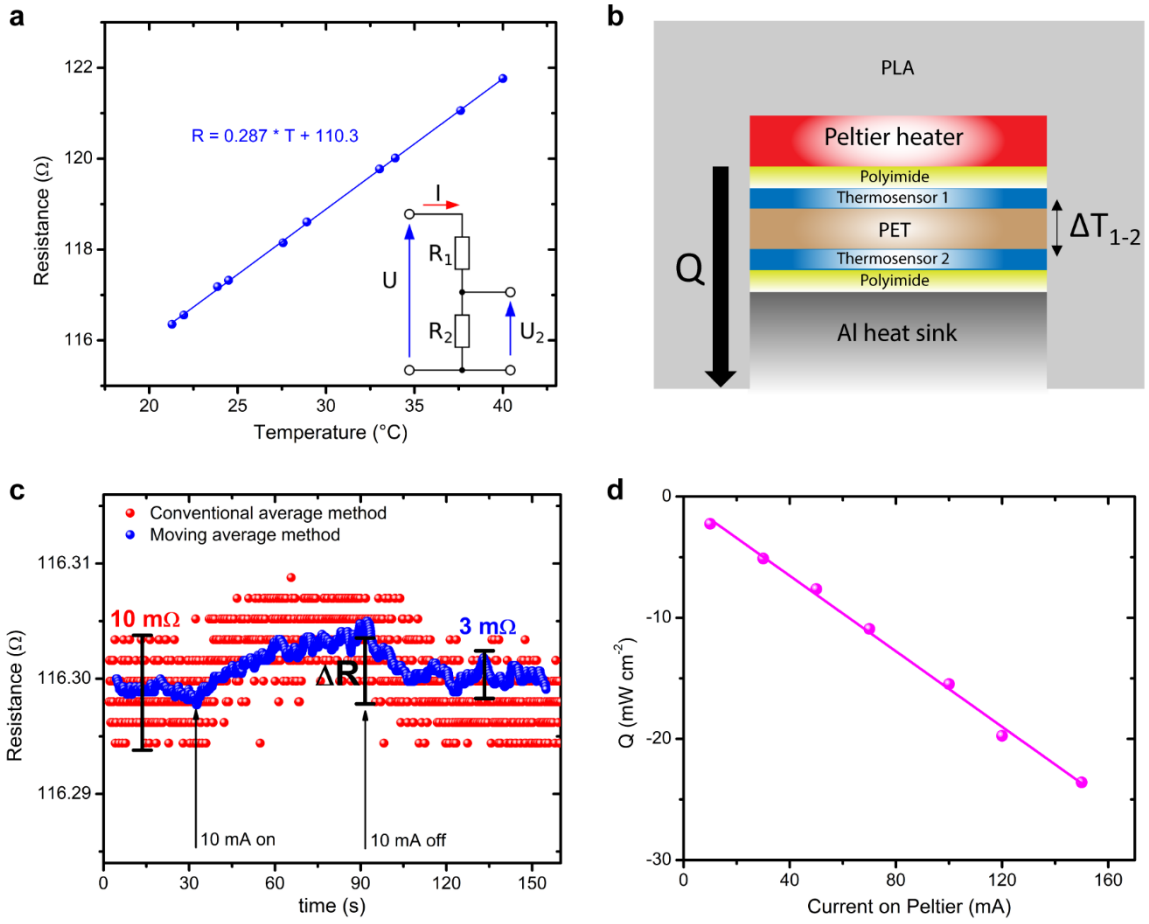

Figure 2. a) Resistance versus temperature measured for the printed resistance temperature sensor. The inset shows the voltage divider used for the measurement of the resistance R_2. **b**) Schematic representation of the set-up designed to study the influence of the temperature sensor's resistance resolution on its temperature and heat-flux measurement capabilities. **c**) Comparison of the effect of the averaging method on the resolution of the resistance measurement. **d**) Heat flux measured as a function of various current values applied to the Peltier element from 10 mA to 150 mA.

The resistance resolution was then further decreased down to 3 mΩ by using a moving average method instead of a conventional average method. In both cases each data point corresponds to the average measurement over n points. However, in a conventional average method, the first data point is displayed after the n^{th} measurement, as shown in in Fig. S2a for n = 6, then the second data point is displayed after the $2n^{th}$ measurement. This method significantly limits the measurement frequency, which is then divided by n. As a result, only 2 points are displayed after having measured 12 values of resistance in Fig S2a. When using a moving average method, the averaging is done over the n previously measured resistance values, instead of having to measure n new values before averaging. This allows to free the measurement frequency from

n, which can then be set to a much higher value, even for high frequency. Fig. S2b, shows that for n = 6, 7 data points are displayed after having measured 12 values of resistance with a moving average method, compared to only two data points in the case of a conventional average method. The influence of the averaging method on the resistance resolution is shown in Fig. 2c, where the time dependence of the resistance of the temperature sensor 2 is measured at 10 Hz with both methods. With the conventional averaging method, each data points corresponds to the average over 6 resistance values (n = 6), which result in the previously mentioned resistance resolution of 10 mΩ. However, using the moving average method, it was possible to increase sixteen-fold the number of resistance values for each data point (n = 96), while keeping the same measurement frequency. As a result, the resistance resolution was decreased from 10 mΩ to 3 mΩ. This resistance resolution corresponds to the targeted temperature resolution of 10 m°C with the printed temperature sensor. To illustrate the impact of this resolution enhancement, a current generating a small heat flux was applied to the Peltier heater at 30 s and then removed 60 s later. As the temperature sensor 2 is the furthest away from the Peltier element, it withstands the smallest temperature-induced change in resistance. Fig. 2c shows that the resolution provided by the conventional averaging method does not allow for an accurate estimation of the temperature-induced resistance change, only a vague trend of increasing resistance can be observed. However, when using the moving average method, the significantly increased resistance resolution allows for an accurate measurement of the change in resistance, even for such a small current applied to the Peltier heater. While better *TCR* have been achieved recently, especially in reduced graphene oxide (rGO) based sensors,[20,21,24] a resolution of 10 m°C ranks among the best reported performance in flexible sensors, as shown in Table 1.

Table 1. Comparison of the performance indicators of our printed sensors with reported temperature sensors using different sensing materials.

Sensing Material	Test Range (°C)	*TCR* (% °C)	Resolution (°C)	Flexibility	Ref.
Ag	22 to 40	0.25	0.01	Yes	This work
Ag	20 to 60	0.22		Yes	[17]
Ag	30 to 100	0.10		Yes	[18]
Pt	25 to 115	0.21		Yes	[8]
Pt	20 to 120	0.32		Yes	[19]
rGO	25 to 45	1.3	0.1	Yes	[20]
rGO	30 to 80	1.34	0.2	Yes	[21]
rGO	25 to 43	0.62		Yes	[24]
Graphene	20 to 50	1.34	5	Yes	[25]
Graphene	30 to 80	0.62	5	No	[26]

The scalability and the flexibility of these printed sensors, in which the performances were found to be maintained upon bending at various angles (Fig. S3), provide them with a wide variety of potential applications. In addition to temperature data, using two temperature sensors with overlapping area and a substrate with known thermal conductivity gives access to the heat flux Q through the substrate as

$$Q = \frac{\Delta T_{1-2}}{R_{PET}} = \frac{A\, K_{PET}\, \Delta T_{1-2}}{d_{PET}}$$

Where $\Delta T_{1\text{-}2}$ is the temperature difference between the temperature sensor 1 and the temperature sensor 2 and R_{PET} the thermal resistance of the reference PET substrate, with d_{PET} the thickness and A the active surface area. The thermal conductivity of the reference PET substrate was measured using the transient plane heat source (hot disc) method[27] (ISO 22007-2) and found to be K_{PET} = 0.147 W K^{-1} m^{-1}. Fig. 2d displays the heat flux measured as a function of various current values applied to the Peltier element. It shows that the temperature resolution of the temperature sensors allowed the measurement of heat fluxes as small as 2 mW cm^{-2}. This range of accessible heat flux values opens the door to a wide variety of potential applications. For instance, Ma *et al.* recently reported a flexible electrocaloric cooler based on self-actuation[3], in

which the smallest heat flux that they required to measure was ~ 2 mW cm^{-2}. Although their design and its performance were promising, they added that the bulky heat flux sensor that they used for the measurement had a detrimental effect on the actuation. Printing our high-resolution temperature sensor directly on the flexible cooler would bypass this issue and provide the actual cooling performance of the device.

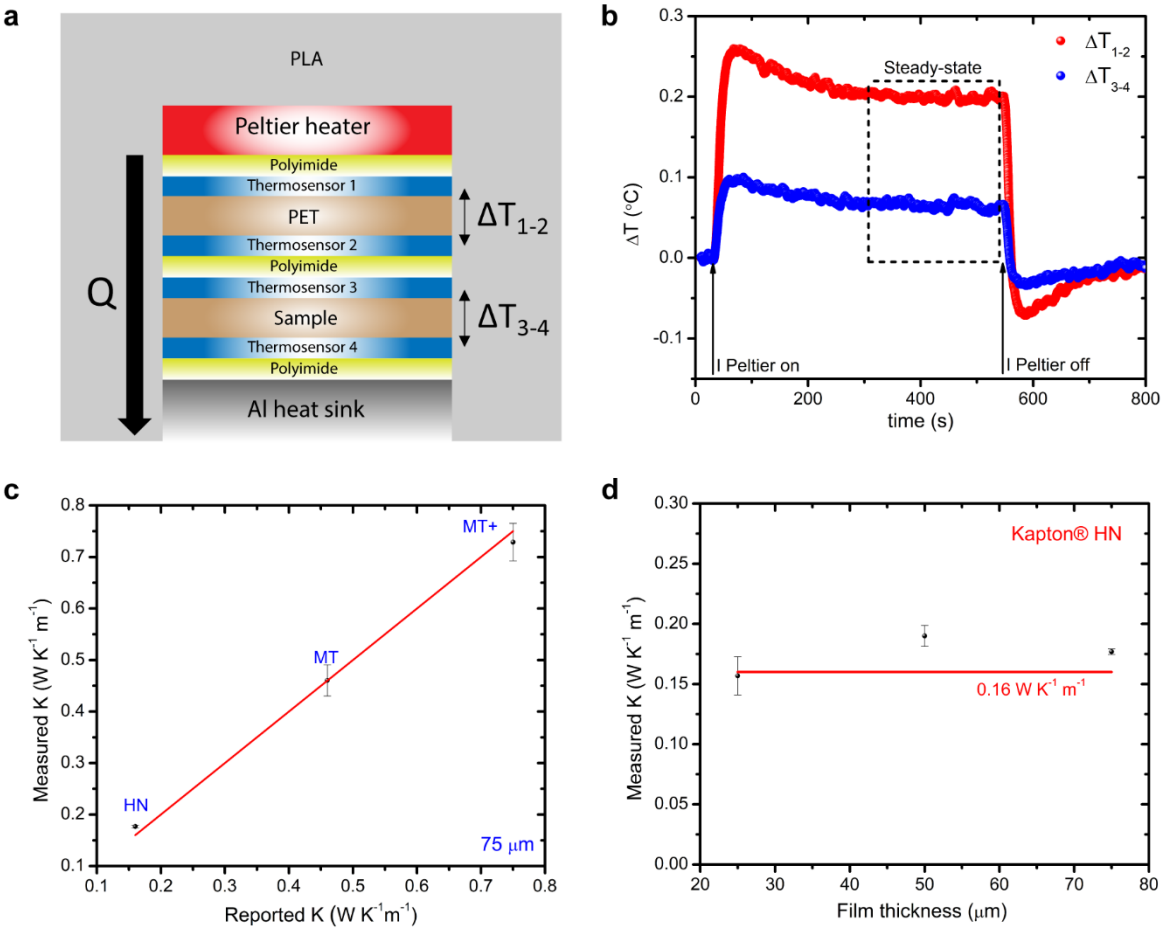

Figure 3. **a**) Schematic representation of the set-up designed to measure the thermal conductivity of a polymer film using four printed temperature sensors. **b**) Temperature gradients measured through a 75-µm-thick Kapton MT sample and the 75-µm-thick reference PET, $\Delta T_{3\text{-}4}$ and $\Delta T_{1\text{-}2}$ respectively, when a 37 mW cm^{-2} heat flux is applied with the Peltier heater at 22 °C. **c**) Measured thermal conductivity versus reported values for various 75-µm-thick polyimide films: Kapton HN, Kapton MT and Kapton MT+. The red line has a slope of 1. **d**) Measured thermal conductivity versus film thickness for polyimide Kapton HN.

This technology could also be used to measure the thermal conductivity of polymer films with a steady-state method. It can be achieved by printing temperature sensors on the polymer

sample of interest and mounting it in series with a material of known thermal conductivity, on which another set of temperature sensors has been printed, and then flowing heat through the multi-stacks, as shown in Fig. 3a, where PET is used as the reference material. The temperature gradients for a given heat flux are then measured. This approach is thus similar to the commonly used comparative cut-bar technique.[28] Fig. 3b shows the temperature gradients through a 75-µm-thick DuPont Kapton MT sample and the 75-µm-thick reference PET, $\Delta T_{3\text{-}4}$ and $\Delta T_{1\text{-}2}$ respectively, when a 37 mW cm^{-2} heat flux is applied with the Peltier. After 300 s the steady-state is established and the heat flux is constant so that

$$Q = Q_{1-2} = Q_{3-4}$$

, the thermal conductivity of the sample can thus be extracted as

$$\frac{K_{PET}\,\Delta T_{1-2}}{d_{PET}} = \frac{K_{sample}\,\Delta T_{3-4}}{d_{sample}}$$

In these conditions, the thermal conductivity of Kapton MT, K_{MT}, was found to be 0.46 ± 0.03 W K^{-1} m^{-1}, which is good agreement with the values reported by the manufacturer for this polymer of 0.46 W K^{-1} m^{-1}. Several commercial polyimides with various thermal conductivities were characterised with this method and the results were compared with values provided by the manufacturers. 75-µm-thick films of DuPont Kapton HN, Kapton MT and Kapton MT+ were selected, with reported thermal conductivities of 0.16 W K^{-1} m^{-1}, 0.46 W K^{-1} m^{-1} and 0.75 W K^{-1} m^{-1} respectively.[29] A good agreement was found for all these polymers, as shown in Fig. 3c. As expected the error bar increased with the thermal conductivity of the sample, from ± 0.01 W K^{-1} m^{-1} for Kapton HN to ± 0.04 W K^{-1} m^{-1} for Kapton MT+. This is due to the lower temperature gradient induced through this more conductive materials, which was closer to the detection limit of the temperature sensors for Kapton MT+. However, the quality of the measurement was assured by adapting the value of the heat flux applied during the measurement, from 20 to 60 mW cm^{-2} depending on the thermal resistance of the sample, in order to maintain $\Delta T_{3\text{-}4} > 0.06$ °C, which was thus six times higher than the thermal resolution of 0.01 °C.

This method was also used to measure the thermal conductivity of films with various thicknesses. Satisfactory results were obtained for films as thin as 25 µm with a measured value for Kapton HN of 0.16 ± 0.02 W K^{-1} m^{-1} compared with an average reported value of 0.16 W K^{-1} m^{-1}, as shown in Fig. 4d, where the comparison is given for three different thicknesses (25 µm, 50 µm and 75 µm) of Kapton HN. These results further highlight the high quality and versatility of the measurements performed with these printed temperature sensors.[30]

CONCLUSIONS

In summary, we have designed and produced a temperature sensor, which can be printed on flexible substrates including PET, PEN and PI. The choice of a silver particle ink offers an alternative to expensive commercial platinum sensors, with the added benefit of the use of easily scalable screen-printing. By combining a highly-sensitive silver micro-pattern with an advanced signal treatment based on a moving average data acquisition, we were able to reach a 10 m°C thermal resolution. By designing an adapted testing system with 3D-printing, we have demonstrated the versatility of our temperature sensor and its potential for a wide variety of applications, including in-situ heat flux measurements, where a 2 mW cm^{-2} resolution was reached, and thermal conductivity measurements on polymer films as thin as 25 µm, with a wide range of accessible values from ~ 0.1 to 0.8 W K^{-1} m^{-1}.

ASSOCIATED CONTENT

Supporting Information

Supporting Information is available free of charge from the American Chemical Society or from the authors. Included are the experimental details; a detailed description of the electronic setup used to measure the resistance values of up to four printed resistance temperature sensors; a

description of the averaging method used for the measurements; and measurements of the resistance of the flexible printed temperature sensors upon bending with different curvature angles.

AUTHOR INFORMATION

Corresponding Authors

Florian Le Goupil - Laboratoire de Chimie des Polymères Organiques (LCPO UMR 5629), Université de Bordeaux, CNRS, Bordeaux INP, 16 Avenue Pey-Berland, 33607 Pessac Cedex, France

Email: florian.le-goupil@u-bordeaux.fr

Georges Hadziioannou - Laboratoire de Chimie des Polymères Organiques (LCPO UMR 5629), Université de Bordeaux, CNRS, Bordeaux INP, 16 Avenue Pey-Berland, 33607 Pessac Cedex, France

Email: georges.hadziioannou@u-bordeaux.fr

Authors

Guillaume Payrot - ELORPrintTec, Allée Geoffroy Saint-Hilaire, F-33600, Pessac, France

Email: payrot@adera.fr

Sokha Khiev - ELORPrintTec, Allée Geoffroy Saint-Hilaire, F-33600, Pessac, France

Email: skhiev@enscbp.fr

Wiljan Smaal - ELORPrintTec, Allée Geoffroy Saint-Hilaire, F-33600, Pessac, France

Email: wiljan.smaal@u-bordeaux.fr

Notes

The authors declare no conflict of interest.

ACKNOWLEDGMENTS

This work was performed within the framework of the Equipex ELORPrintTec ANR-10-EQPX-28-01.

REFERENCES

(1) Rogers, J. A.; Someya, T.; Huang, Y. Materials and Mechanics for Stretchable Electronics. *Science.* **2010**, *327* (5973), 1603–1607. https://doi.org/10.1126/SCIENCE.1182383.

(2) Su, Y.; Ma, C.; Chen, J.; Wu, H.; Luo, W.; Peng, Y.; Luo, Z.; Li, L.; Tan, Y.; Omisore, O. M.; et al. Printable, Highly Sensitive Flexible Temperature Sensors for Human Body Temperature Monitoring: A Review. *Nanoscale Res. Lett.* **2020**, *15* (1), 1–34. https://doi.org/10.1186/S11671-020-03428-4.

(3) Ma, R.; Zhang, Z.; Tong, K.; Huber, D.; Kornbluh, R.; Ju, Y. S.; Pei, Q. Highly Efficient Electrocaloric Cooling with Electrostatic Actuation. *Science* **2017**, *357* (6356), 1130–1134. https://doi.org/10.1126/science.aan5980.

(4) Arman Kuzubasoglu, B.; Kursun Bahadir, S. Flexible Temperature Sensors: A Review. *Sensors Actuators, A Phys.* **2020**, *315*. https://doi.org/10.1016/J.SNA.2020.112282.

(5) Tai, H.; Duan, Z.; Wang, Y.; Wang, S.; Jiang, Y. Paper-Based Sensors for Gas, Humidity, and Strain Detections: A Review. *ACS Appl. Mater. Interfaces* **2020**, *12* (28), 31037–31053. https://doi.org/10.1021/ACSAMI.0C06435.

(6) Mattana, G.; Briand, D. Recent Advances in Printed Sensors on Foil. *Mater. Today*

2016, *19* (2), 88–99. https://doi.org/10.1016/J.MATTOD.2015.08.001.

(7) Barmpakos, D.; Kaltsas, G. A Review on Humidity, Temperature and Strain Printed Sensors—Current Trends and Future Perspectives. *Sensors* **2021**, *21* (3), 739. https://doi.org/10.3390/S21030739.

(8) Lee, G.; Wu, J.; Miau, J. A New Fabrication Process for a Flexible Skin with Temperature Sensor Array. *J. Chin. Inst. Engin.* **2002**, *25* (6), 619–625. https://doi.org/10.1080/02533839.2002.9670736.

(9) Bowden, N.; Brittain, S.; Evans, A. G.; Hutchinson, J. W.; Whitesides, G. M. Spontaneous Formation of Ordered Structures in Thin Films of Metals Supported on an Elastomeric Polymer. *Nat.* **1998**, *393* (6681), 146–149. https://doi.org/10.1038/30193.

(10) Liu, P.; Zhu, R.; Que, R. A Flexible Flow Sensor System and Its Characteristics for Fluid Mechanics Measurements. *Sensors* **2009**, *9* (12), 9533–9543. https://doi.org/10.3390/S91209533.

(11) Nur, H. M.; Song, J. H.; Evans, J. R. G.; Edirisinghe, M. J. Ink-Jet Printing of Gold Conductive Tracks. *J. Mater. Sci. Mater. Electron.* **2002**, *13* (4), 213–219. https://doi.org/10.1023/A:1014827900606.

(12) Cummins, G.; Kay, R.; Terry, J.; Desmulliez, M. P. Y.; Walton, A. J. Optimization and Characterization of Drop-on-Demand Inkjet Printing Process for Platinum Organometallic Inks. *2011 IEEE 13th Electron. Packag. Technol. Conf. EPTC 2011* **2011**, 256–261. https://doi.org/10.1109/EPTC.2011.6184427.

(13) Wang, Y.-F.; Sekine, T.; Takeda, Y.; Yokosawa, K.; Matsui, H.; Kumaki, D.; Shiba, T.; Nishikawa, T.; Tokito, S. Fully Printed PEDOT:PSS-Based Temperature Sensor with High Humidity Stability for Wireless Healthcare Monitoring. *Sci. Reports* **2020**, *10* (1), 1–8. https://doi.org/10.1038/s41598-020-59432-2.

(14) Aliane, A.; Fischer, V.; Galliari, M.; Tournon, L.; Gwoziecki, R.; Serbutoviez, C.; Chartier, I.; Coppard, R. Enhanced Printed Temperature Sensors on Flexible Substrate.

Microelectronics J. **2014**, *45* (12), 1621–1626. https://doi.org/10.1016/J.MEJO.2014.08.011.

(15) Menon, H.; Aiswarya, R.; Surendran, K. P. Screen Printable MWCNT Inks for Printed Electronics. *RSC Adv.* **2017**, *7* (70), 44076–44081. https://doi.org/10.1039/C7RA06260E.

(16) Thuau, D.; Kallitsis, K.; Dos Santos, F. D.; Hadziioannou, G. All Inkjet-Printed Piezoelectric Electronic Devices: Energy Generators, Sensors and Actuators. *J. Mater. Chem. C* **2017**, *5* (38), 9963–9966. https://doi.org/10.1039/C7TC02558K.

(17) Dankoco, M. D.; Tesfay, G. Y.; Benevent, E.; Bendahan, M. Temperature Sensor Realized by Inkjet Printing Process on Flexible Substrate. *Mater. Sc. Engin. B* **2016**, *205*, 1. https://doi.org/10.1016/j.mseb.2015.11.003

(18) Liew, Q. J.; Lee, H. W. Inkjet-Printed Flexible Temperature Sensor Based on Silver Nanoparticles Ink. *Eng. Proc.* **2020**, *2* (3), 8216. https://doi.org/10.3390/ECSA-7-08216.

(19) Lee, G. Bin; Huang, F. C.; Lee, C. Y.; Miau, J. J. New Fabrication Process for a Flexible Skin with Temperature Sensor Array and Its Applications. *Acta Mech. Sin.* **2004**, *20* (2). https://doi.org/10.1007/bf02484257.

(20) Liu, Q.; Tai, H.; Yuan, Z.; Zhou, Y.; Su, Y.; Jiang, Y. A High-Performances Flexible Temperature Sensor Composed of Polyethyleneimine/Reduced Graphene Oxide Bilayer for Real-Time Monitoring. *Adv. Mater. Technol.* **2019**, *4* (3). https://doi.org/10.1002/admt.201800594.

(21) Trung, T. Q.; Ramasundaram, S.; Hwang, B. U.; Lee, N. E. An All-Elastomeric Transparent and Stretchable Temperature Sensor for Body-Attachable Wearable Electronics. *Adv. Mater.* **2016**, *28* (3). https://doi.org/10.1002/adma.201504441.

(22) Molina-Lopez, F.; Quintero, A. V.; Mattana, G.; Briand, D.; De Rooij, N. F. Large-Area Compatible Fabrication and Encapsulation of Inkjet-Printed Humidity Sensors on

Flexible Foils with Integrated Thermal Compensation. *J. Micromechanics Microengineering* **2013**, *23* (2), 25012. https://doi.org/10.1088/0960-1317/23/2/025012.

(23) Ali, S.; Hassan, A.; Bae, J.; Lee, C. H.; Kim, J. All-Printed Differential Temperature Sensor for the Compensation of Bending Effects. *Langmuir* **2016**, *32* (44), 11432–11439. https://doi.org/10.1021/ACS.LANGMUIR.6B02885/SUPPL_FILE/LA6B02885_SI_001.AVI.

(24) Salvo, P.; Calisi, N.; Melai, B.; Cortigiani, B.; Mannini, M.; Caneschi, A.; Lorenzetti, G.; Paoletti, C.; Lomonaco, T.; Paolicchi, A.; et al. Temperature and pH Sensors Based on Graphenic Materials. *Biosens. Bioelectron.* **2017**, *91*. https://doi.org/10.1016/j.bios.2017.01.062.

(25) Zhao, X.; Long, Y.; Yang, T.; Li, J.; Zhu, H. Simultaneous High Sensitivity Sensing of Temperature and Humidity with Graphene Woven Fabrics. *ACS Appl. Mater. Interfaces* **2017**, *9* (35). https://doi.org/10.1021/acsami.7b09184.

(26) Nguyen, D. K.; Kim, T. Y. Graphene Quantum Dots Produced by Exfoliation of Intercalated Graphite Nanoparticles and Their Application for Temperature Sensors. *Appl. Surf. Sci.* **2018**, *427*. https://doi.org/10.1016/j.apsusc.2017.09.020.

(27) ISO - ISO 22007-2:2015 - Plastics — Determination of thermal conductivity and thermal diffusivity — Part 2: Transient plane heat source (hot disc) method https://www.iso.org/standard/61190.html (accessed Oct 17, 2022).

(28) Zhao, D.; Qian, X.; Gu, X.; Jajja, S. A.; Yang, R. Measurement Techniques for Thermal Conductivity and Interfacial Thermal Conductance of Bulk and Thin Film Materials. *J. Electron. Packag. Trans. ASME* **2016**, *138* (4). https://doi.org/10.1115/1.4034605.

(29) DuPont Kapton https://www.dupont.com/electronic-materials/kapton-polyimide-

film.html (accessed Oct 17, 2022).

(30) Katerinopoulou, D.; Zalar, P.; Sweelssen, J.; Kiriakidis, G.; Rentrop, C.; Groen, P.; Gelinck, G. H.; van den Brand, J.; Smits, E. C. P. Large-Area All-Printed Temperature Sensing Surfaces Using Novel Composite Thermistor Materials. *Adv. Electron. Mater.* **2019**, *5* (2), 1800605. https://doi.org/10.1002/AELM.201800605.

For Table of Contents Only